Assessment of Salt and Acid Droplets Evaporations on the Corrosion Mechanism of Aluminum

Gamal A. EL-Mahdy[1,2] Mohammed Abdel-Reheem[3,4] and Omar M.EL-Roudi[2], Ayman M. Atta[1, 5],
,Zuheir Issa[1], Hamad A. Al-Lohedan[1]

[1]Surfactant Research Chair, Department of Chemistry, College of Science, King Saud University, Riyadh 11451, Kingdom of Saudi Arabia.
[2]Chemistry Department, Faculty of Science, Helwan University, Helwan, Egypt
[3]Research Center, College of Science, King Saud University, Riyadh, Saudi Arabia
[4]Biochemistry Department, Faculty of Agriculture, Ain Shams University, Cairo, Egypt
[5] Petroleum application department, Egyptian petroleum research institute, Nasr city 11727, Cairo, Egypt.
[*]E-mail: gamalmah2000@yahoo.com

An approach for new experimental set up for monitoring the corrosion rate of aluminum along with the contact angle, droplet volume loss and droplet height of a single droplet of NaCl , NH_4SO_4, H_2SO_4 and HNO_3 solutions placed gently on aluminum surface was suggested. Electrochemical impedance spectroscopy (EIS) technique was employed for monitoring the corrosion rate, while the contact angles, volume loss and droplet height changes were monitored using drop shape analyzer. The evaporation process for the droplets from aluminum surface is followed and characterized. The evaporation of droplet is highly dependent upon the reaction of salt and acid with exposed aluminum surface, which is important for monitoring the contact angle and droplet height. The constancy of the base diameter determines the evaporation mode of the droplet. The change in a contact angle shows a remarkable decrease with droplet holding time. The corrosion process of aluminum is mainly dependent upon droplet height. The volume losses increase, while the droplet height decreases as droplet holding timer progressed. A mechanism describing the corrosion process inside the droplet is suggested.

1. INTRODUCTION

Inkjet printing[1-2], microfluidic lab-on-a-chip processes [3-4], phase-change cooling, [5-6] and controlled deposition of self-assembled surface coatings [7-8] are considered as different

applications based on the Evaporation   process of sessile droplets on a solid substrate. The participation of the substrate with liquid during the evaporation process changing the shape of the droplet. Wetting has received growing interest in many industrial processes, such as corrosion, printing, spray quenching, oil recovery and lubrication, [9–14]. Several techniques have been established for contact angle measurement, such as the adhering gas bubble method (15), Wilhelm plate method, the capillary penetration techniques (16-17) and the sessile drop technique (18-19). Contact angle measurement is highly dependent upon water content [20-23], surface roughness [24–26], temperature [27–29], relative humidity [30], particle size [14] surface heterogeneity [31–33] and cations [34-35]. The diffusion of the liquid vapor is limited owing to the presence of the substrate, which constrains the evaporation process. Contact angle provides valuable information about surface roughness, heterogeneity and polymer surface dynamics [36-42] and considered as complicated and multifaceted phenomena [43-44]. Chemical reactions between solid and liquid play an important role in determination of the contact angle. Shanahan et al [38-39] observed   the constancy of the contact radius during evaporation process of liquid drops placed on polymer and glass surfaces. The drop height and the contact radius diminish concurrently and keeping contact angle more or less constant for smooth surfaces and does not occur on irregular surfaces [38]. Local interfacial evaporation flux and the total evaporation rate could be employed for a droplet with any arbitrary contact angle with Popov's model for vapor diffusion-based solutions [45]. The effect of deviations from a spherical cap of droplet shape on the evaporation rate have been examined by Erbil et al [46-47]. They reported that the initial contact angle can be determined by the rate of evaporation [48-49]. The previous vapor diffusion-based models were improved by Dunn et al [50]. The predictions of the evaporation rate and residual mass at any time of the drop based on the spherical cap geometry have been developed by Picknett and Bexon [51]. Aluminum has enormous application in industries among the other nonferrous metals [52]. Atmospheric corrosion is characterized by the most failures in terms of cost and tonnage among the other environment [53].The total annual corrosion costs in the U.S. aircraft industry have been estimated at several billion dollars [54]. Aluminum is the most applicable metal in the atmosphere especially in building and aerospace industries among the other metals [55-56]. In addition to atmospheric corrosion, aluminum suffers different forms of corrosion as filiform corrosion [57], exfoliation corrosion [48], intergranular corrosion [49], and pitting corrosion [58-60]. The effect of NaCl, NH_4Cl, NH_4SO_4, Na_2SO_4 and RH on corrosion rate of aluminum have been investigated previously [61-63]. The extensive use of aluminum alloys in the automobile industry and construction may be attributed to high strength-to-weight ratio and high corrosion resistance [64-66]. Aluminum is a metal frequently exposed to the atmosphere in many practical applications, especially in building and aerospace industries [67-68]. Many researchers and groups have been extensively investigated the atmospheric corrosion of aluminum alloys in outdoors exposures [69-71]. The most widely used as an acceleration test [72-74] among the conventional laboratory scale tests is the salt spray test (ASTM B117) [75-76]. Simulation of actual atmospheric corrosion at a laboratory level has been conducted using cyclic corrosion tests, such as ASTM G85-A5 and SAE J2334 [77-78]. The severity of atmospheric corrosion depends on the environment type [79]. There has no been studies on the simultaneous monitoring of the corrosion rate under a single droplet along with droplet characteristics. The present work suggests a new experimental set up for assessment the corrosion rate of aluminum

under a single droplet of NaCl , NH_4SO_4, H_2SO_4 and HNO_3 solution and proposes a mechanism describing the corrosion process of aluminum inside the droplet.

## 2. EXPERIMENT PROCEDURE

2.1. Materials preparation

Aluminum sheets were used sized 10mm (length) x 1mm width). Two plates were connected with copper wire using silver paste and secured with quick dry epoxy. The plates were placed 0.1mm apart from each other and fixed in an epoxy resin. The samples were abraded with silicon carbide paper down to 2000 mesh before each experiment.

2.2. AC impedance measurements and Contact angle measurements

EIS experiment was conducted at 10 kHz (ZH) and 10 mHz (ZL) using a Solartron 1280. The calculation of the polarization resistance (Rp) is based on monitoring the impedance at low frequency (10 kHz) and high frequency (10 mHz). Contact angles, Volume loss, droplet height and Base diameter were determined with the sessile drop method using Drop Shape Analysis System, DSA100 (Krüss GmbH, Hamburg, Germany) .

3. RESULTS AND DISCUSSION

3.1 Evolution of contact angle
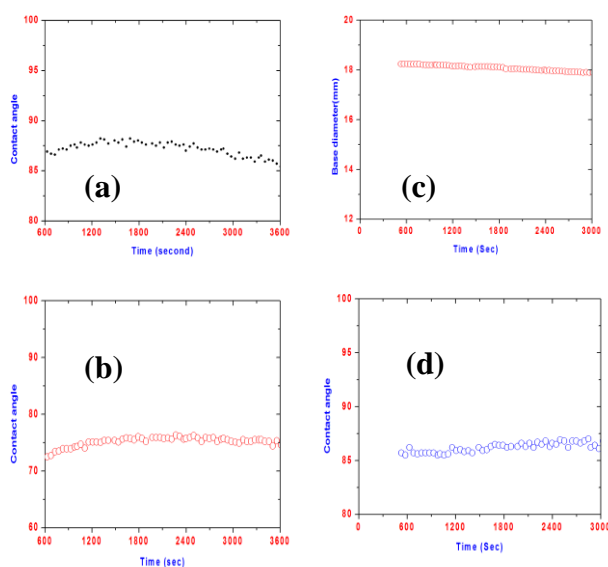
Figure 1. Monitoring data of contact angle with time under a single droplet of (a) NaCl (b) NH_4SO_4 (c) H_2SO_4 (d) HNO_3

The corrosion process of the metals under thin electrolyte layers was conducted under constant thickness and concentration of the tested electrolyte [79-83]. In case of outdoors exposures of metals the concentration and thickness of the thin electrolyte layer on a metal surface continuously change due to water evaporation or adsorption. The acid rain led to formation of droplet with different contact angles and volumes on the exposed surface, which creates the corrosion process of the underlying surface. Figures 1a, 1b, 1c and 1d show the evolution of contact angle (CA) with time for single droplet of NaCl and NH4SO4 , H2SO4 and HNO3 solution, respectively. Contact angle decrease linearly with time as a result of the evaporation process of acid droplets placed over aluminum surface. The interaction of the investigated droplet with the substrate led to lowering the CA as the volume losses increases. As a result of this interaction, the properties of the solid/liquid interface will be changed and affect the value of CA. The decrease in CA can be explained on the basis of transport of tested liquid from the drop to the liquid/vapor interface and to a decrease in the number of adsorption centers. The weak binding between the droplet and the substrate enhances the evaporation of the tested liquid from the aluminum surface and consequently increase the volume losses of the tested liquid.

The results also can be accounted to a continuous evaporation of water molecules. The evaporation process occurs in three different stages. The constant mode of evaporation with constant base diameter resulted in a decrease in contact angle. The water molecules diffuse out from aluminum surface and are accompanied by a slight change in the base diameter with small fluctuations in contact angle values. During the initial measurements the contact angle is slightly decreased in the period before droplet completely dried up. A decrease in the contact angle is generally expected as holding time progressed. The evaporative flux at the liquid/air interface is uniform, and the evaporation proceeds more quickly as this interface becomes larger. The precipitation of the corrosion products over the surface increases the resistance to the contact generally expected as holding time progressed. The evaporative flux at the liquid/air interface is uniform, and the evaporation proceeds more quickly as this interface becomes larger. The precipitation of the corrosion products over the surface increases the resistance to the contact line motion. It can be concluded that a lesser amounts of corrosion products at the solid/liquid interface produces a low resistance to the contact line motion. The contact angle measurement is significantly dependent on the chemical reactivity of the aluminum with droplet composition, which causes a change in the liquid-vapor surface. Increasing the contact angle led to an increase in the contact of the tested electrolyte with aluminum surface and hence enhances the corrosion rate. The increase in the concentration of the tested electrolytes due to evaporation significantly affects the corrosion rate of aluminum. The results are in consistent with that reported previously [84-85].

3.2 Evolution of droplet volume, height and base diameter

The experimental data for the volume loss and the droplet height during the course of droplet evaporation is shown in Figures 2a, 2b 2c and 2d for single droplet of NaCl and NH4SO4 , respectively. Figures 3a, 3b 3c and 3d show the experimental data for the volume loss and the droplet

height during the droplet evaporation H_2SO_4 and HNO_3 solution, respectively. It can be seen from Figures 3-6   that the droplet height decreases, while volume losses increases as holding time progresses. The results can be explained on the basis of the evaporation process of tested electrolyte, which increases as time increases. The evaporation process is increasing closer to the contact line and the electrolyte is flowing toward to the contact line to compensate the evaporated solvent. Three phases can be observed during the evaporation process of the acid droplet. A saturation of the surrounding atmosphere around the acid droplet has been attained during the first phase in a very short time. The droplet base diameter is a constant during the second phase. The droplet base diameter is a constant during the second phase and the volume loss increases linearly with time. The droplet height decreased rapidly with increasing the volume loss during the third phase of evaporation.
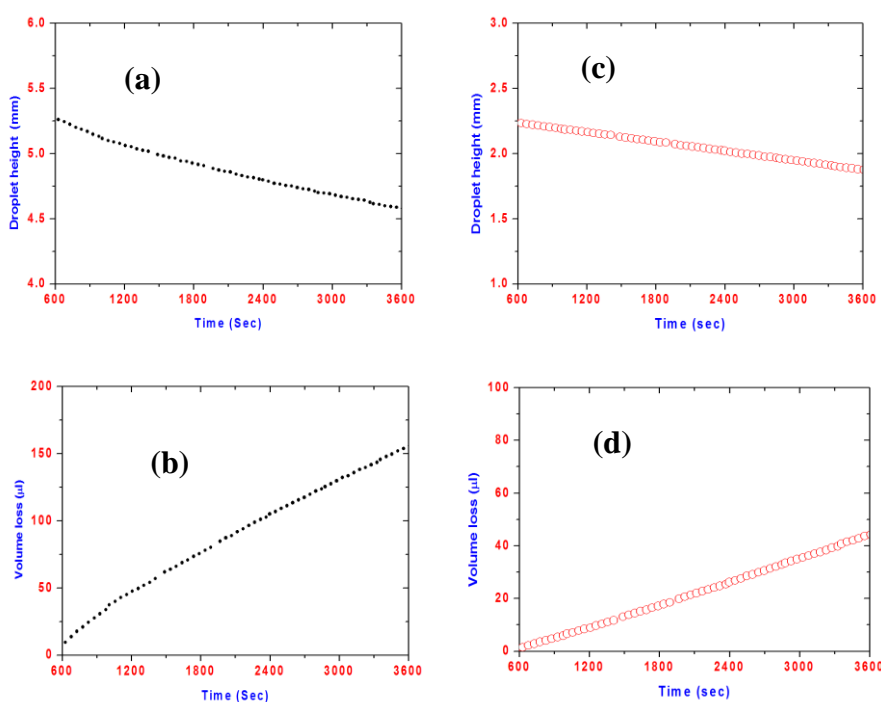
Figure 2. Monitoring data of: (a) Droplet height for NaCl   (b) volume loss with time for NaCl (c) Droplet height for NH_4SO_4 (d) volume loss with time for NH_4SO_4.

The length of each phase is determined by a chemical reactivity between the aluminum surface and the droplet. In addition, the constancy of the base diameter during the initial stage of evaporation enables the liquid vapor to diffuse out along the contact line. It is evident that the base diameter was slightly changed and almost constant through the whole evaporation in both acids. During the last stage of drying process the solvent is completely dried up from the substrate. The particles are carried by the electrolyte flow toward the drop contact line, which causes accumulation and deposition of particles above the substrate. The droplet height has a significant effect on the cathodic reduction of oxygen. Evaporation of the electrolyte led to a decrease in the droplet height, which provide shorter path for the diffusion of oxygen. This will accelerate the corrosion process of aluminum, which is

mainly controlled by cathodic reduction of oxygen [86]. Evaporation of the tested electrolyte also led to a decrease in the volume and size of the droplet, which in turn decreases the number of the formed anode and cathode on the exposed aluminum surface and consequently lowered the corrosion process of aluminum [87]. Masuda reported that the decrease in the size of the droplet is accompanied by a decrease in the area of the interface, which give rise to more difficulties in the formation of a defined anode and cathode and hence reduce the corrosion rate [88].

3.3 Mechanism of Aluminum corrosion under a single droplet

The polarization resistance of aluminum was monitored with droplet holding time. It was established that the corrosion rate is proportional to the reciprocal of polarization resistance and can be calculated according to Stern–Geary equation [89]:

$$\text{Corrosion rate} = K/Rp \qquad (1)$$
$$K = b\text{a} \times b\text{c} / 2.303(b\text{a} + b\text{c}) \qquad (2)$$

where ba and bc are anodic and cathodic Tafel slopes, respectively. The value of K can be assumed to be a constant for a given metal–electrolyte system [90-91]. Monitoring data of $1/Rp$ versus time is shown in Fig.4 for NaCl, Fig. 5 for NH_4SO_4 , Fig. 6 for H_2SO_4 and Fig. 7 for HNO_3 solutions. The corrosion process can be divided into two distinct regions.
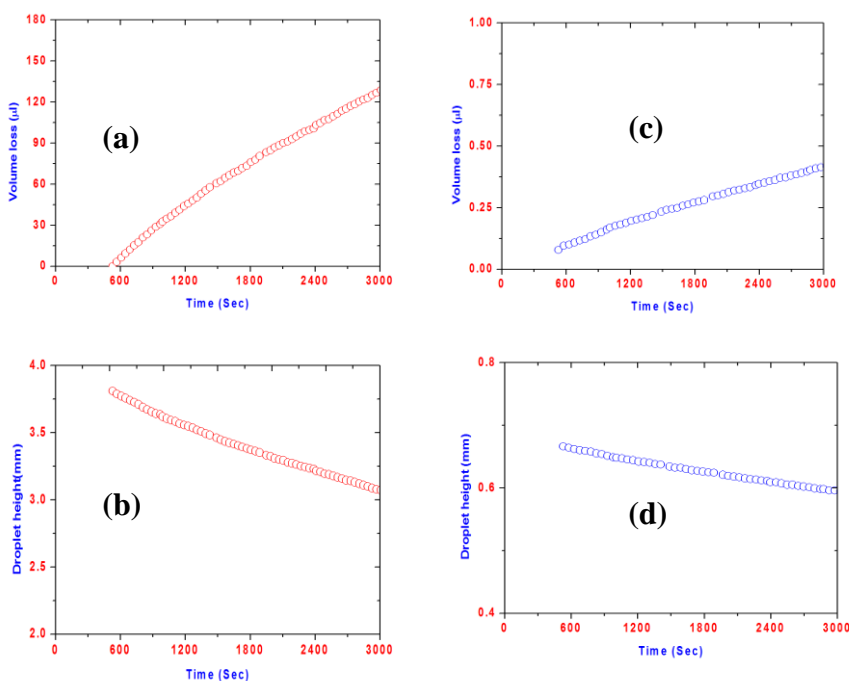
Figure 3. Monitoring data of: (a) Droplet height for H_2SO_4. (b) volume loss with time for H_2SO_4. (c) Volume loss with time for HNO_3 (d) Droplet height for HNO_3

The corrosion rate increases slowly during the initial immersion of the drying period region I (from zero time to 30 min), then sharply increases during the end of drying period in region II (from 30 time to 60 min) as the holding drying time progress. The corrosion reaction under a single droplet of can be divided into two stages with the transitions from the one stage to the next occurring at aluminum surface as droplet holding time progresses. The mechanism of aluminum corrosion inside NaCl droplet can be explained by low and high corrosion processes. The slow rate of corrosion experienced during the onset of drying period in region I can be attributed to dissolution of native oxide film followed by aluminum dissolution when droplet height is high as shown in the inset of Figure 7 and 8 (top), which shows the sequences of droplet shape at different holding times. This behavior is similar to the anodic dissolution of aluminum in NaCl bulk solution. The formation of aluminum corrosion products above the aluminum surface leads to a decrease in the corrosion rate as time progresses. The relatively high corrosion rate observed in region II was attributed to an increase in NaCl concentration due to the evaporation of electrolyte as drying time progresses leads to enhancement of the corrosion rate. In addition, the evaporation of the electrolyte leading to a decrease in the thickness of electrolyte as the drying time progressed, which enhances the diffusion of oxygen through a short path of electrolyte with low droplet height and increase the reduction process of oxygen. The most abundant ions in fine dust particles commonly found in urban environments are ammonium and sulfate ions. The data presented in Figure 8 for NH_4SO_4 droplet indicated that the value of $1/Rp$, decreased rapidly in the initial stage of monitoring due to the rapid dissolution of Al_2O_3 followed by aluminum dissolution. The slow increase in corrosion rate during the last stage of monitoring can be attributed to the precipitation of ammonium aluminum sulfate $(NH_4)_3Al(SO4)_3$ as given below [92]:

$$Al^{+3} + (NH4)_2SO4 \rightarrow (NH4)_3Al(SO4)_3 + 3NH_3^{+3} + 2H_2 \qquad (3)$$

Aluminum initially tarnishes rapidly due to their increased chemical reactivity to form a protective oxide layer. The natural aluminum oxide layer can protect the aluminum from atmospheric corrosion. Aluminum is characterized by a formation of an insulating oxide film and is liable to dissolution process in the acidic media. The passivation or formation of protective film is highly dependent upon the chemical reactivity of the formation medium towards the aluminum [93]. The underlying aluminum surface started to dissolve in the acidic solution and the corrosion of the aluminum is controlled by the anodic and cathodic reactions. The anodic dissolution of aluminum can be described as [94]:

$$4Al = 4Al^{3+} + 12e^{-3} \qquad (4)$$

The cathodic reduction of hydrogen proceeds as [38-39]:

$$3O_2 + 12H^+ + 12e^{-1} = 6H_2O \qquad (5)$$

The corrosion rate in this stage is initially high and controlled by anodic dissolution of Al in the acidic solution and decreases as time progresses. The contact angle, and droplet height also decreases linearly, while the volume losses increases due to evaporation of the acidic droplet. The aluminum dissolution in case of H_2SO_4 solution can be described as:

$$Al + 3H^+ = Al^{3+} + 3/2H_2 \qquad (6)$$

In case of HNO_3 the reaction may occur as [46]:

$$Al + 4H^+ + NO_3^- = Al^{3+} + NO + 2H_2O \qquad (7)$$
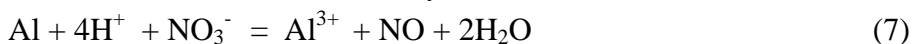
The liberation of aluminum started after an induction period from the contact of the droplet with the surface. This time can be defined as the time required for complete dissolution of the oxide film and followed by dissolution of the underlying surface of aluminum [95-96]. In H_2SO_4, the sulfates ions have a strong affinity to adsorb water on the aluminum surface and resist the aluminum dissolution [97]. In HNO_3, there are two competing processes, the first is the oxide film growth and the second process is the Al dissolution. Both processes are highly dependent upon acid concentration. In high concentration, the former process is dominant process and the latter process is dominating process in low concentration. A previous study indicated that increasing the HNO_3 concentrations enhances the passive film formation on aluminum surface [98]. In addition, the formation rate of passive film is higher than that dissolution one. The corrosion rate of the oxide film formation in diluted HNO_3 solution is higher than that experienced in high concentrated HNO_3 solution. The results may be attributed to lower degree of protectiveness of the formed oxide film in diluted solution of HNO_3 [99]. Gaseous products as NO, NH3 and N2 as well as soluble ions as NH_4 and NO^{-2} may be formed as corrosion products [100]. It was established previously that an increase in nitric concentration is accompanied by an enhancement of aluminum dissolution [46,69]. The results indicated that the rate of aluminum dissolution may be attributed to a formation of a complex, which increases with increasing nitric concentration.
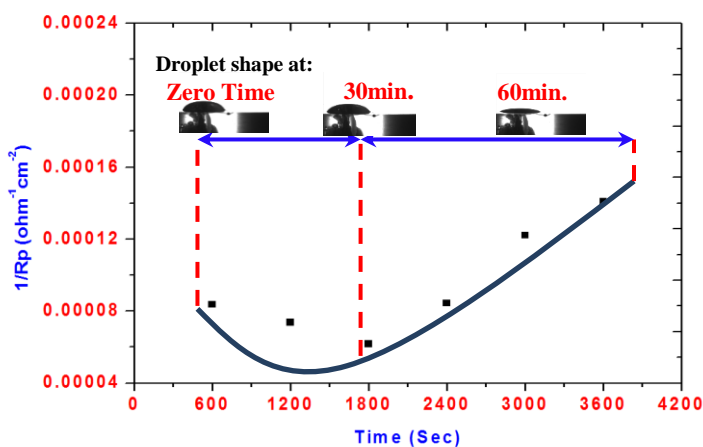

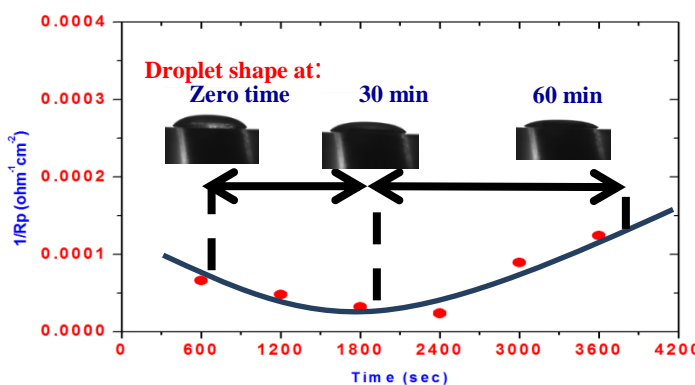**Figure 4.** Monitoring data of 1/Rp versus time for NaCl.

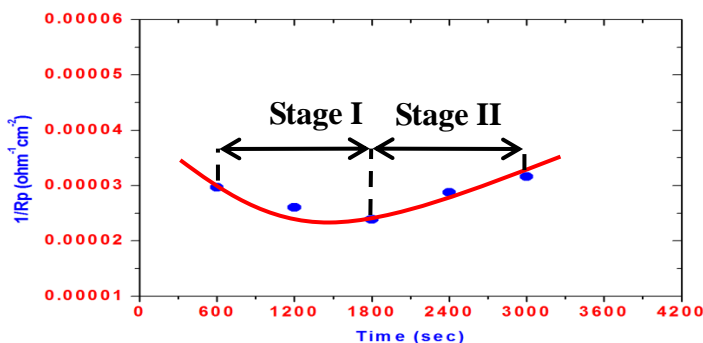**Figure 5.** Monitoring data of 1/Rp versus time for NH_4SO_4

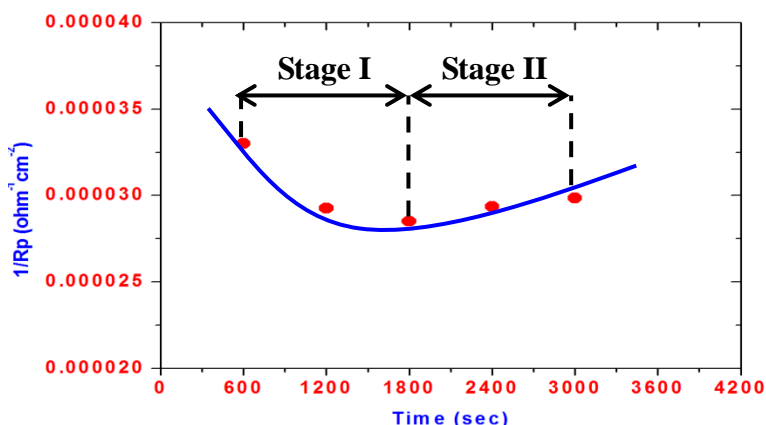**Figure 6.** Monitoring data of 1/Rp versus time for H_2SO_4

Figure 7. Monitoring data of 1/Rp versus time for HNO_3 .

The photomicrograph of aluminum surface after complete drying is shown in Fig. 8(a-d) for NaCl, NH_4SO_4 , H_2SO_4 and HNO_3 solutions, respectively. It can be concluded that the corrosion process is anodically controlled by anodic dissolution of aluminum with a high droplet height and is cathodically controlled by reduction of oxygen when the droplet height is small.

4. CONCLUSIONS

1. The experimental set up employed in this study is useful in monitoring the corrosion rate along with volume loss, droplet height and contact angle under a single droplet of aqueous solution.

2. Droplet height and contact angle decrease with droplet holding time while volume losses increases

3. The acid wetting and spreading on aluminum surface depends on the roughness and chemical reactivity of the aluminum surface.

4. The evaporation of droplet is highly dependent upon the reaction of acid with exposed aluminum surface.

5. Droplet height plays an important role in controlling the corrosion process of aluminum.

6. The mechanism of the corrosion process inside the droplet changed from anodically controlled process during the initial stage of immersion to cathodically controlled process during the last stage monitoring.
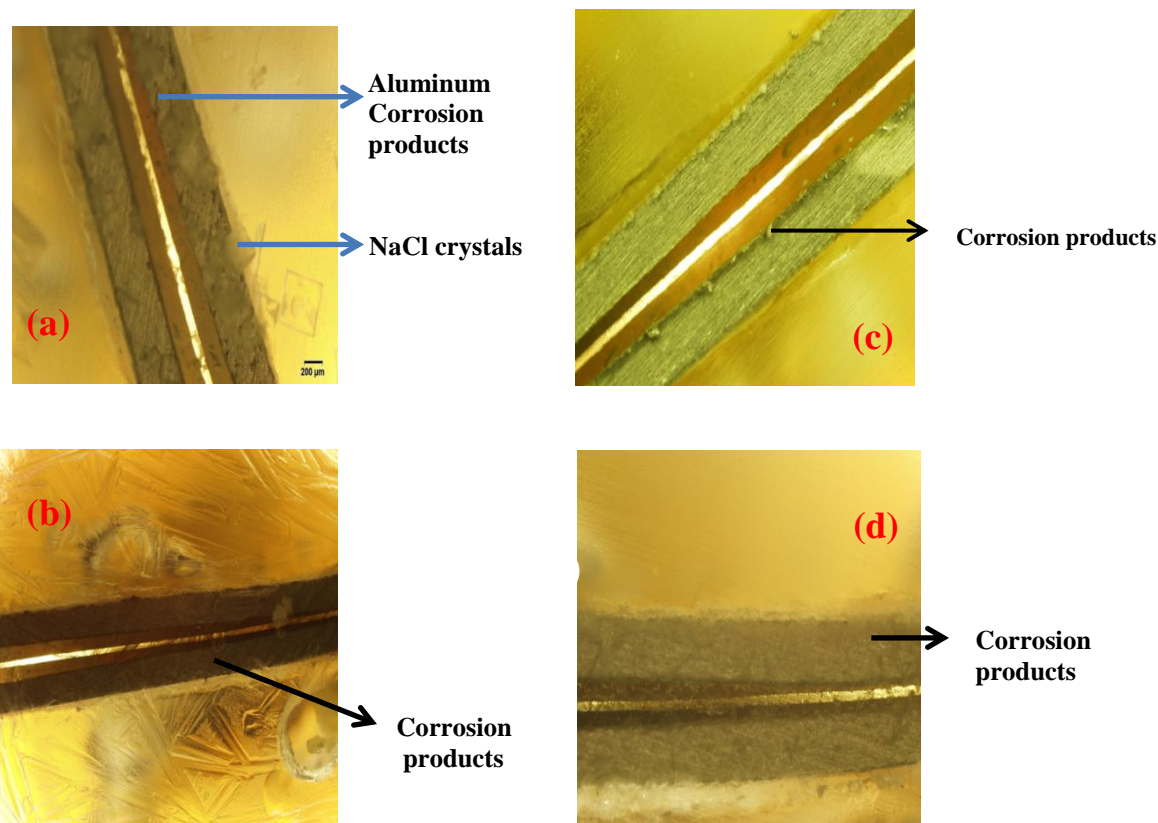
Figure 8. Photomicrograph of aluminum surface after complete drying of: (a) NaCl droplet. (b) NH$_4$SO$_4$ droplet (c) H$_2$SO$_4$ droplet (d) HNO$_3$ droplet

References

1. M. Singh, H. M. Haverinen, P. Dhagat, G. E. Jabbour, *Adv. Mater*., 22 (2010) 673.
2. T. Lim, S. Han, J. Chung, J. T Chung, S. Ko, C. P. Grigoropoulos, *Int. J. Heat Mass Transfer,* 52 (2009) 431.
3. N. J. Carroll, S. B. Rathod, E. Derbins, S. Mendez, D. A. Weitz, D. N. Petsev, *Langmuir,* 24 (2008) 658.
4. S. T. Chang, O. D. Velev, *Langmuir,* 22 (2006)1459.
5. N. Kumari,S. V. Garimella, *Int. J. Heat Mass Transfer,* 54 (2011) 4037.
6. W.L.Cheng, F.Y Han, Q.-N Liu, R. Zhao, H. Fan, *Energy,* 36 (2011) 249.
7. Á. G. Marín,H. Gelderblom, D. Lohse, J. H. Snoeijer, *Phys. Rev. Lett.,* 107 (2011)085502.
8. S. Zhang, Li, Q. I. A. Kinloch, A.H. Windle, *Langmuir,* 26 (2009) 2107.

9. K.N. Prabhu, P. Fernandes, G. Kumar, *Mater. Des.*, 2 (2009) 297.
10. X. Zhao, M. J. Blunta, J. J. Yao, *Pet. Sci. Technol. Eng.*, 71 (2010) 169.
11. Y. Q. Wang, H. F. Yang, Q.G. Hang, L. Fang, S.R. Ge, *Adv.Mater. Res.*, 154–155 (2010) 1019.
12. M. Sakai, T. Yanagisawa, A. Nakajima, Y. Kameshima, K. Okada, *Langmuir,* 25 (2009) 13.
13. Y. Son, C. Kim, D. H. Yang, D.J. Ahn, *Langmuir,* 24 (2008) 2900.
14. J. Perelaer, C.E. Hendriks, A.W.M. de Laat, U.S. Schubert, *Nanotechnology*, 20 (2009) 165303.
15. E Gyorvary, J. Peltonen, M. Linden, and J.B. Rosenholm, *Thin Solid Films,* 284 (1996) 368.
16. M.S. Rosen, *Surfactants and Interfacial Phenomena,* 2nd edn., John Wiley & Sons, New York, 1989, pp. 224, 240.
17. T.V Subrahmanyam, C.A. Prestidge, and J. Ralston, *Miner. Eng.*, *9*:727 (1996).
18. A.W., Adamson, *Physical Chemistry of Surfaces*, 5th edn., John Wiley & Sons, New York, 1990, p. 379.
19. C. Serre, P. Wynblatt, and D. Chatain, *Surf. Sci.*, 415 (1998) 336.
20. L.W. DeJonge, O.H. Jacobsen, P. Moldrup, *Soil Sci. Soc. Am. J.*, 63 (1999) 437.
21. L.W. Dekker, C.J. Ritsema, *J. Hydrol.*, 231 (2000) 148.
22. L.W. deJonge, P. Moldrup, O.H. Jacobsen, *Soil Sci.*, 172 (2007) 577.
23. J. Bachmann, M. Deurer, G. Arye, *Vadose Zone., J.* 6 (2007) 436.
24. J. Eick, R. Good, A. Neumann, *J. Colloid Interface Sci.*, 53 (1975) 235.
25. J. Oliver, C. Huh, S. Mason, *Colloids Surf.,* 1 (1980) 79.
26. J. Drelich, J. Miller, R. Good, J. *Colloid Interface Sci.*, 179 (1996) 37.
27. P.M. King, *Aust. J. Soil Res.*, 19 (1981) 275–285.
28. L.W. Dekker, C.J. Ritsema, K. Oostindie, O.H. Boersma, *Soil Sci.*, 163 (1998) 780.
29. H.Y. She, B. Sleep, *Water Resour. Res.*, 34 (1998) 2587.
30. P. Chassin, C. Jounay, H. Quiquampoix, *Clay Miner.*, 21 (1986) 899.
31. R.E.J. Johnson, R.H. Dettre, Contact angle hysteresis. III. *J. Phys. Chem.*, 68 (1964) 1744.
32. R.H. Dettre, R.E.J. Johnson, Contact angle hysteresis. IV. *J. Phys. Chem.*, 69 (1965) 1507.
33. J. Long, M. Hyder, R. Huang, P. Chen, *Adv. Colloid Interface Sci.*, 118 (2005) 173.
34. R.F. Giese, C.J. van Oss, Colloid and Surface Properties of Clays and Related Minerals, *CRC Press*, *Oxford*, 2002.
35. E. Chibowski, M.L. Kerkeb, F. Gonzlez-Caballero, *Langmuir,* 9 (1993) 2491.
36. Á. G Erbil, Surface Tension of Polymers. In Handbook of Surface and Colloid Chemistry; Birdi, K. S., Ed.; CRC Press Inc.: Boca Raton, FL, 1997; Chapter 9, pp 259-306.
37. M. Morra, E. Occhiello, F. Garbassi, *AdV. Colloid Interface Sci.*, 32 (1990) 79.
38. R. J. Good, Contact Angle, Wettability and Adhesion; K. L. Mittal, Ed.; VSP: Utrecht, 1993; pp 3-36.
39. R. E. Johnson, R. H. Dettre, *J. Phys. Chem.*, 68 (1964) 1744.
40. P. G. De Gennes, *Mod. Phys.*, 57 (1985) 827.
41. M. E. R. Shanahan, *J. Phys. D: Appl. Phys.,* 22 *(*1989) 1128.
42. J. D Andrade, M. Gregonis, L. Smith, . *Physicochem. Aspects Polym. Surf., 2* (1985) 911
43. M. E. R. Shanahan, C. Bourges, *Int. J. Adhesion Adhesives.,* *14* (1994) 201.
44. M. C. Bourges, M. E. R. Shanahan, *Langmuir,* 11 (1995) 2820.
45. Y. O Popov, *Phys. Rev., E* 71 (2005) 036313.
46. H. Y Erbil, R. A Meric, *J. Phys. Chem., B* 101 (1997) 6867.
47. R. A Meric, H. Y Erbil, *Langmuir,* 14 (1998)1915.
48. H. Y Erbil, *J. Phys. Chem., B 102* (1998) 9234.
49. H. Y. Erbil, *J. Adhes. Sci. Technol.,* 13 (1999)1405.
50. G. Dunn, S.Wilson, B. Duffy, S. David, K. Sefiane, *J. Fluid Mech.*, 623 (2009) 329.
51. R. G. Picknett, R. Bexon, *J. Colloid Interface Sci., 61* (1977) 336.
52. Schweitzer, P.: Fundamentals of metallic corrosion: atmospheric and media corrosion of metals. CRC press (2007) ISBN 0849382432, P. 250- 280.

53. S. L. Pohlman, "Atmospheric Corrosion," Metals Handbook, 9th ed., Vol. 13, ASM International, Metals Park, OH, 1987, pp. 80-83.
54. V. S. Agarwala, P. K. Bhagat, and G. L. Hardy, "Corrosion Detection and Monitoring of Aircraft Structures: An Overview," AGARD Conference Proceedings 565, Corrosion Detection and Management of Advanced Airframe Materials, Seville, Spain, October 1994.
55. R. T. Foley, *Corrosion*, 42 (1986) 277.
56. R. Z. Nakazato, E. N. Codaro, L. M. F. Ribeiro, L. R. O. Hein, *Prakt. Metallogr.*, 38 (2001) 301.
57. J. A. González, M. Morcillo, E. Escudero, V. López, E. Otero, *Surf. Coat. Technol.*, 153 (2002) 225.
58. R. Vera, D. Delgado, B. M. Rosales, *Corros. Sci.*, 48 (2006) 2882.
59. A.S. Elola, T. F. Otero, A. Porro, *Corrosion*, 48 (1992) 854.
60. D. Bengtsson Blücher, J.E. Svensson, L.- G. Johansson, *Corros. Sci.*, 48 (2006) 1848.
61. M. Natesan, G. Venkatachari, N. Palaniswamy, *Corros. Sci.*, 48 (2006) 3584.
62. D. de la Fuente, E. Otero-Huerta, M. Morcillo, *Corros. Sci.*, 49 (2007) 3134.
63. W.S. Patterson, J.H. Wilknson, *J. Soc. Chem. Ind.*, 57 (1938) 445.
64. J.H. Wilknson, W.S. Patterson, *J. Soc. Chem. Ind.*, 60 (1938) 42.
65. B. Saynayl, D.V. Bahadwar, *J. Sci. Ind. Res.* 21D (1962) 243.
66. J. R. Davis. ASM Specialty Handbook: Aluminium and Aluminium Alloys. In: ASM International, Metals Park, OH, USA, 1993, p8-55.
67. R. T. Foley, *Corrosion*, 42 (1986) 277.
68. R. Z. Nakazato, E. N. Codaro, L. M. F. Ribeiro, L. R. O. Hein, *Prakt. Metallogr.*, 38 (2001) 301.
69. F. L. McGeary, T. J. Summerson, W. H. Ailor , Atmospheric Exposure of Nonferrous Metals and Alloys-Aluminium: Seven-Year Data, Metal Corrosion in the Atmosphere, ASTM STP 435, American Society for Testing and Materials, 1968. p141-174.
70. J. J. Friel. *Corrosion, 42* (1986) 422.
71. T. E. Graedel . *J. Electrochem. Soc.*, 136 (1989) 204C.
72. D. de la Fuente., E. Otero-Huerta., M . Morcillo. *Corros. Sci.,* 49 (2007) 3134.
73. D.B. Blücher., R. Lindström , J.E. Svensson JE., L. G. Johansson. *J. Electrochem. Soc.,* 148(2001) B127.
74. S.B. Lyon., G.E. Thompson., J.B. Johnson . *Corrosion,* 43 (1987)719.
75. Y . Shi., Z. Zhang.,J. Su., F. Cao ., J. Zhang. *Electrochim. Acta,* 51 (2006) 4977.
76. G. A El-Mahdy., K. B. Kim. *Electrochim. Acta,* 2004;49:1937.
77. F. Deflorian , S. Rossi , S. Prosseda . *Mate. Des.*, 2006;27:758.
78. A. Nazarov ,D. Thierry *Electrochim. Acta,* 2004;49:2717.
79. G.A. El-Mahdy, A. Nishikata, T. Tsuru, *Corros. Sci.*, 42 (2000) 1509.
80. A. Nishikata, Y. Ichihara, T. Tsuru, *Electrochim. Acta* ,41 (1996) 1057.
81. A. Nishikata, Y. Ichihara, T. Tsuru, *J. Electrochem. Soc.*, 144 (1997) 1244.
82. Y.L. Cheng, Z. Zhang, F.H. Cao, J.F. Li, J.Q. Zhang, J.M. Wang, C.N. Cao, *Corros. Sci.,* 46 (2004) 1649.
83. Y.Y. Shi, Z. Zhang, Y.L. Cheng, F.H. Cao, J.Q. Zhang, J.M. Wang, C.N. Cao, *Bull. Electrochem.* ,20 (2004) 261
84. R. Wang and M. Kido SCRIPTA MATER, 55 (2006) 633.
85. G A. EL-Mahdy, Amro K.F. Dyab, Ayman M. Atta , Hamad A. Al-Lohedan, *Int. J. Electrochem. Sci.,* 8 (2013) 9992.
86. 1. J.F. Li, B. Maier, G.S. Frankel,*Corros. Sci.,* 53 (2011) 2142.
87. H. Masuda, *Corrosion*, 57 (2001) 99.
88. J.R. Vilche, F.E. Varela, G. Acuna, E.N. Codaro, B.M. Rosales, A. Fernandez, G. Moreina, *Corros. Sci. ,* 37 (1995) 941.
89. M. Stern, A.L. Geary, *J. Electrochem.*, 104 (1957) 56.
90. G.A. EL-Mahdy, A. Nishikata, T. Tsuru, *Corros. Sci.*, 42 (2000) 183.

91. G.A. EL-Mahdy, *Corrosion,* 59 (2003) 505.
92. R.E. Lobing, D.J. Siconolfi, J. Maisano, G. Grundmeier, H. Streckel, R.P. Frankenthal, M. Stratmann, J.D. Sinclair, *J. Eletcrochem. Soc.*,143 (1996) 1175.
93. A. Santos, L. Vojkuvka, J. Pallarés, J. Ferré-Borrull, L.F. Marsal *J. Electroanal. Chem.*, 632 (2009) 139.
94. Sastri, V.; Ghali, E.; M. Elboujdaïni: Corrosion prevention and protection: practical solutions. John Wiley & Sons (2007) ISB N047002402X, P. 50-85.
95. Ghali, e.; Revie, R.: Corrosion Resistance of Aluminum and Magnesium Alloys. Wiley-VCH (2010) ISBN 978-0-471-71576-4, P. 31-43.
96. Davis, J.; Corrosion: understanding the basics. ASM International (2000) ISBN 0871706415, P. 120-155. 57. Bardal, E.: Corrosion and protection. Springer-Verlag London Limited (2004) ISBN 1852337583, P. 110-120.58.
97. S.M. Abd El Haleem, S. Abd El Wanees, E.E. Ab El Aal, A. Farouk, *Corros. Sci.,* 68 (2013) 1.
98. M.S. Hunter, P. Fowle, *J. Electrochem. Soc.*, 103 (1956) 482.
99. J. Flis, K. Kowalczyk, *J. Appl. Electrochem.*, 25 (1995) 501–507.
100. S.S. Kim, W.J. Lee, S.I. Pyun, D.R. Kim, *Met. Mater.*, 5 (1999) 583–588.